

Self-focusing of elliptic beams: an example of the failure of the aberrationless approximation

G. Fibich and B. Ilan

School of Mathematical Sciences, Tel Aviv University, Tel Aviv 69978, Israel

Received May 23, 1999

We show that the increase in critical power for elliptic input beams is only 40% of what had been previously estimated based on the aberrationless approximation. We also find a theoretical upper bound for the critical power, above which elliptic beams always collapse. If the power of an elliptic beam is above critical, the beam self-focuses and undergoes partial beam blowup, during which the collapsing part of the beam approaches a circular Townesian profile. As a result, during further propagation additional small mechanisms, which are neglected in the derivation of the nonlinear Schrödinger equation (NLS) from Maxwell's equations, can have large effects, which are the same as in the case of circular beams. Our simulations show that most predictions for elliptic beams based on the aberrationless approximation are either quantitatively inaccurate or simply wrong. This failure of the aberrationless approximation is related to its inability to capture neither the partial beam collapse nor the subsequent delicate balance between the Kerr nonlinearity and diffraction. We present an alternative two-stage approach and use it to analyze the effect of nonlinear saturation, nonparaxiality, and time dispersion on the propagation of elliptic beams. The results of the two-stage approach are found to be in good agreement with NLS simulations. © 2000 Optical Society of America [S0740-3224(00)02009-9]

OCIS codes: 190.3270, 190.5940, 260.5950.

1. INTRODUCTION

The propagation of intense laser beams in a medium with Kerr nonlinearity is one of the classic problems in nonlinear optics. The effect of ellipticity of the input beam on beam propagation was considered by Giuliano *et al.*¹ To analyze the nonlinear Schrödinger equation (NLS) for beam propagation they used the aberrationless approximation, i.e., the assumption that the beam maintains a Gaussian shape during propagation:

$$|E|^2 = \frac{E_0^2}{a^*(z)b^*(z)} \exp\left\{-\left[\frac{x}{a^*(z)}\right]^2 - \left[\frac{y}{b^*(z)}\right]^2\right\}, \quad (1)$$

where $a^*(z)$ and $b^*(z)$ are the beam widths in the x and y directions, respectively. Using this assumption, they reduced the NLS to a system of two coupled ordinary-differential equations for $a^*(z)$ and $b^*(z)$. The reduced system was used to predict that the critical power of collimated beams will increase with ellipticity e as

$$P_{\text{cr}}(e) = h(e)P_{\text{circular}}, \quad h(e) = \frac{e + 1/e}{2}, \quad (2)$$

where $e = b^*(0)/a^*(0)$ and P_{circular} is the critical power of the corresponding circular beam. This result was later rediscovered in Ref. 2, where it was pointed out that the increase in critical power can be used to transfer more power through a Kerr medium. In subsequent studies the aberrationless approximation was used in analysis of the propagation of elliptic beams in the presence of additional effects, such as nonlinear saturation, time dispersion, and graded refractive index.³⁻⁵ In none of those studies,¹⁻⁵ however, were the predictions of the aberrationless approximation compared with simulations of the original NLS.

Application of the aberrationless approximation in NLS analysis goes back to the early days of self-focusing research⁶ and was most likely motivated by the case of linear propagation, in which input Gaussian beams maintain a Gaussian profile during propagation. Over the years it became clear that predictions based on the original aberrationless paraxial-approximation method of Ref. 6 can be quantitatively inaccurate as well as qualitatively incorrect.⁷⁻⁹ As a result, various modifications were suggested, such as use of a variational approach (the variational method or the collective coordinate approach)⁹ and replacement of the Gaussian ansatz with super-Gaussians¹⁰ or with a sech profile.⁹ These methods are sometimes called the aberrationless paraxial approximation, the variational method, and the collective coordinate approach. All these methods, however, are based on the aberrationless approximation, i.e., the assumption that the beam maintains the same shape during propagation.

Gross and Manassah¹¹ studied the validity of the aberrationless approximation for elliptic beams, both for the aberrationless paraxial approximation method and for the variational method. Their study pointed to significant differences between quantitative predictions of the aberrationless approximation and actual results obtained in NLS simulations. In addition, they found out that elliptic beams are transformed into circular beams with propagation, a finding that is in qualitative disagreement with predictions of the aberrationless approximation.

In this study we use numerical simulations of the NLS in $(2 + 1)$ dimensions to study further the propagation of elliptic beams in Kerr media. In addition, we provide what we believe is the first comparison of predictions of the aberrationless approximation for elliptic beams propagating in Kerr media in the presence of additional

small mechanisms, with simulations of the corresponding perturbed NLS. Our results show that most predictions of the aberrationless approximation are either quantitatively inaccurate or qualitatively incorrect. We identify the inherent weaknesses of the aberrationless approximation assumption and present an alternative two-stage method for analyzing the propagation of elliptic beams. Although most of this paper is dedicated to elliptic beams, our criticism of the aberrationless approximation as well as of the alternative two-stage method applies also for circular beams.

The paper is organized as follows: In Section 2 we calculate numerically the critical power for elliptic beams. Our calculations show that the increase in critical power is much smaller than that predicted by the aberrationless approximation.² In Section 3 we show that this discrepancy is related to the fact that the aberrationless approximation assumes whole-beam collapse, whereas self-focusing beams undergo partial-beam collapse. In Section 4 we show that the profile of the collapsing part of the beam is close to a modulated Townesian. As a result, there is a delicate balance between diffraction and nonlinearity that the aberrationless approximation is too crude to capture. In Section 5 we present a two-stage approach to the propagation of elliptic beams and use it to analyze the effect of nonlinear saturation, nonparaxiality, and time dispersion. Unlike those of the aberrationless approximation, the predictions of the two-stage method are found to be in good agreement with NLS simulations.

2. CRITICAL POWER

The nonlinear optical process of self-focusing sets an upper limit on the amount of laser power that can be propagated through a Kerr medium (i.e., $n = n_0 + n_2 I$, where n_0 is the linear refractive index, n_2 is the nonlinear refractive index, and I is the intensity). For power above this threshold the beam undergoes catastrophic collapse, with the peak intensity becoming sufficiently high to damage the material. Although the exact value of the critical power depends on the spatial distribution of the input beam, the critical power for beams with circular input profiles is typically not more than a few percent above the theoretical lower bound value $P_{\text{cr}}^{\text{lb}}$ of Eq. (7) below.¹²

We now consider the critical power of elliptic beams. For a scalar monochromatic field $E(x, y, z, t) = A(x, y, z)\exp(ik_0 z - \omega_0 t)$, the propagation of a laser beam in a Kerr medium is governed by

$$2ik_0 A_z + \Delta_{\perp} A + 4\epsilon_0 c k_0^2 n_2 |A|^2 A = 0, \\ \Delta_{\perp} = \partial_{xx} + \partial_{yy},$$

where $k_0 = \omega_0 n_0 / c$ is the wave number and

$$A(x, y, 0) = A_0(\sqrt{(x/a^*)^2 + (y/b^*)^2})$$

is the amplitude of the input elliptic beam. We change to nondimensional variables:

$$\tilde{x} = x/r_0, \quad \tilde{y} = y/r_0, \quad \tilde{z} = z/2L_{\text{df}}, \\ \psi(\tilde{x}, \tilde{y}, \tilde{z}) = 2k_0 r_0 \sqrt{c\epsilon_0 n_2} A(x, y, z),$$

where $r_0 = \sqrt{a^*(0)b^*(0)}$ and $L_{\text{df}} = k_0 r_0^2$ is the diffraction length. The input power of the beam is given by

$$P_0 = 2\epsilon_0 n_0 c \int |A_0|^2 dx dy = \frac{\lambda^2}{8\pi^2 n_0 n_2} N_0, \\ N_0 = \int |\psi_0|^2 d\tilde{x} d\tilde{y}. \quad (3)$$

Dropping the tildes yields the NLS for the nondimensional envelope ψ :

$$i\psi_z(x, y, z) + \Delta_{\perp} \psi + |\psi|^2 \psi = 0, \\ \psi(x, y, 0) = \psi_0(x, y), \quad (4)$$

with the elliptic input profile

$$\psi_0(x, y) = cf(\sqrt{(x/a_0)^2 + (y/b_0)^2}), \quad (5)$$

where $a_0 = a^*(0)/r_0$, $b_0 = b^*(0)/r_0$, and c is a constant. Thus the normalized input beam widths satisfy $a_0 b_0 = 1$.

Let us briefly review the rigorous theory on blowup (singularity formation) in the NLS [Eq. (4)]. For more details, see Refs. 13 and 14. The NLS has waveguide solutions of the form

$$\psi = \exp(i\alpha^2 z)\lambda R(\alpha r), \quad r = \sqrt{x^2 + y^2}, \quad (6)$$

where α is a positive constant and $R(r)$, the so-called Townes soliton, is the circular ground-state solution of

$$\left(\frac{\partial^2}{\partial r^2} + \frac{1}{r}\frac{\partial}{\partial r}\right)R - R + R^3 = 0,$$

$$R'(0) = 0, \quad R(\infty) = 0.$$

Solutions of NLS do not blow up if their initial power N_0 is below the critical power N_{cr} , which is equal to the power of the Townes soliton¹⁵:

$$N_{\text{cr}} = 2\pi \int R^2 r dr \approx 2\pi \times 1.8623.$$

Solutions of NLS do blow up, however, if their initial Hamiltonian is negative (see Section 3 below):

$$H_0 = \int |\nabla \psi_0|^2 dx dy - 1/2 \int |\psi_0|^4 dx dy < 0.$$

Therefore, blow up occurs for the elliptic input profile [Eq. (5)] when

$$c^2 > \left(\frac{1}{a^2} + \frac{1}{b^2}\right) \frac{\int |\nabla f|^2 dx dy}{\int |f|^4 dx dy}$$

or

$$\int |\psi_0(x, y)|^2 dx dy > h(e)G[f],$$

where

$$G[f] = \frac{2 \int |f|^2 dx dy \int |\nabla f|^2 dx dy}{\int |f|^4 dx dy}.$$

We recall that $\min_{f(x,y)} G[f] = N_{cr}$ is attained for $f = R(r)$, whereas for all other profiles $G[f]$ is higher.¹⁵ In addition, $h(e)$ attains its minimum at $e = 1$ (circular profile). Therefore the critical power for the elliptic input profile [Eq. (5)] satisfies

$$N_{cr} \leq N_{cr} [cf(\sqrt{(x/a_0)^2 + (y/b_0)^2})] \leq h(e)G[f].$$

Reexpressing the critical power in physical units yields the lower bound for the critical power¹²:

$$P_{cr}^{lb} = \frac{\lambda^2}{8\pi^2 n_0 n_2} N_{cr}, \tag{7}$$

and the upper bound

$$P_{cr}^{ub} = \frac{\lambda^2}{8\pi^2 n_0 n_2} h(e)G[f]. \tag{8}$$

The upper bound [Eq. (8)] implies that for any input profile f and any level of ellipticity e there is always a critical power above which collapse will occur.

To calculate the critical power of elliptic beams, we solve numerically the NLS in (2+1) dimensions [Eq. (4)] with the elliptic initial conditions of Eq. (5). Although blowup is defined as beam intensity becoming infinite in a finite distance, in the nonlinear optics context a more realistic definition is the point when the beam power exceeds the material's breakdown threshold. In our simulations we define collapse as occurring when beam intensity reaches 10^3 times the input peak intensity. We

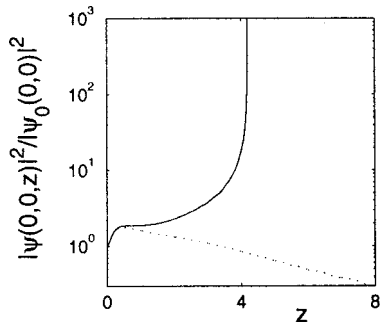


Fig. 1. Normalized on-axis intensity as a function of axial distance for Gaussian beams $\psi_0 = c \exp[-(xe)^2 - y^2]$ with initial ellipticity $e = 1.3$. Blowup occurs when $c = 2\sqrt{0.7872}$ (i.e., $P_0 = 1.015P_{circular}$; solid curve). When $c = 2\sqrt{0.795N_c}$ (i.e., $P_0 = 1.005P_{circular}$; dotted curve), no blowup occurs.

vary the input power until we find a lower power that does not lead to collapse and an upper power that does lead to collapse, whose difference is below $0.01P_{circular}$. For example, for input Gaussian beams with ellipticity $e = 1.3$, blowup occurs when $P_0 = 1.015P_{circular}$, whereas, for $P_0 = 1.005P_{circular}$, collapse is arrested (Fig. 1). Therefore $P_{cr}(1.3) = 1.01P_{circular}$ for Gaussian beams. We remark that in these calculations one has to be careful to set the numerical boundaries sufficiently far from the origin to avoid reflections from the boundaries.

Because $P_{cr}(e) = P_{cr}(1/e)$, in Fig. 2 we plot the critical power as a function of $h(e)$ rather than as a function of e (Ref. 17) for collimated Gaussian, super-Gaussian, and Townesian input beams (the corresponding values of $P_{circular}$ are $1.02P_{cr}^{lb}$, $1.09P_{cr}^{lb}$, and P_{cr}^{lb} , respectively¹²). Our simulations show that, for all three input profiles, the critical power is well approximated¹⁸ by the relation

$$P_{cr}(e) \approx [0.4h(e) + 0.6]P_{circular}. \tag{9}$$

From relation (9) we see that the relative increase in critical power is $0.4[h(e) - 1]$ rather than the predicted $[h(e) - 1]$ of Eq. (2). Thus the increase in critical power that is due to ellipticity is only 40% of what was previously predicted based on the aberrationless approximation.

We recall that the critical power for singularity formation in the NLS is independent of input beam focusing.^{13,16} Therefore, in theory, the value of $P_{cr}(e)$ is independent of the input focusing angle. In practice, however, the critical power for a beam to exceed the material's breakdown threshold does decrease with input beam focusing. However, this decrease is typically so small that, even under this definition, relation (9) can be applied for both collimated and focused beams.

3. PARTIAL-BEAM BLOWUP

To explain the disagreement of relation (2) with the numerical results of relation (9) we first observe that the theoretical upper bound P_{cr}^{ub} of Eq. (8) for the critical power does satisfy Eq. (2). This observation has a simple explanation, as both Eqs. (2) and (8) are derived from the condition that $H_0 = 0$. We thus see that $P_{cr}(e)$ in Eq. (2) is the aberrationless approximation for the theoretical upper bound P_{cr}^{ub} rather than for the actual critical power.

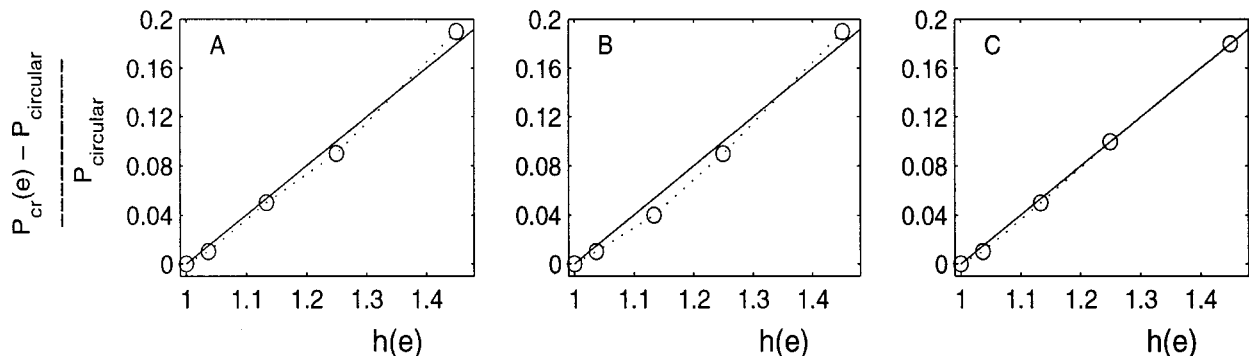


Fig. 2. The increase in critical power with initial ellipticity (dotted curves with circles) is well approximated by relation (9) (solid curves). Input beam profiles are A, Gaussian; B, super-Gaussian; C, Townesian.

Hence the disagreement of Eq. (2) and relation (9) reflects the fact that the upper bound P_{cr}^{lb} is a poor predictor of the actual critical power. The reason for this has to do with the condition that $H_0 = 0$ and not with the effect of ellipticity. Indeed, numerical simulations with circular beams show that the condition $H_0 = 0$ leads to a significant overestimate of the actual critical power. For example, for circular beams with a super-Gaussian profile $\psi_0 = c \exp(-r^4)$, the difference between the actual critical power and the upper bound derived from the condition $H_0 = 0$ is 40%.¹²

To understand the limitations of the condition $H_0 = 0$ we recall that solutions of the NLS satisfy the variance identity¹⁹

$$V_{zz}(z) = 8H_0, \quad V = \int r^2 |\psi|^2 dx dy.$$

Therefore $V(z) = 4H_0 z^2 + V_z(0)z + V(0)$. As a result, when $H_0 < 0$, the function $V(z)$ vanishes at some $z^* > 0$. For example, in the case of collimated beams, $V(z) = 4H_0 z^2 + V(0)$ and

$$V(z^*) = 0, \quad z^* = [V_0/(-4H_0)]^{1/2}. \quad (10)$$

Unfortunately, Eq. (10) has often been misinterpreted to imply the following:

- 1, the blowup point is given by z^* ;
- 2, at the blowup point the whole beam collapses toward its center;
- 3, there is a qualitative difference between collapse when $H_0 < 0$ (whole-beam collapse) and when $H_0 > 0$ (partial-beam collapse); and
- 4, the condition $H_0 = 0$ provides a good estimate of the critical power.

These wrong conclusions are reinforced when the aberrationless approximation assumption is used because then $V(z) = L^2(z)V(0)$ and the variance identity reduces to $(L^2)_{zz}(z) = 8H_0/V_0 = (L^2)_{zz}(0)$. For example, in the case of elliptic beams the aberrationless approximation for the variance identity is $(a^2 + b^2)_{zz}(z) = (a^2 + b^2)_{zz}(0)$ [see Eq. (3) of Ref. 1 and Eq. (5) of Ref. 2]. Therefore, under the aberrationless approximation, the condition $H_0 = 0$ appears to be both necessary and sufficient for blowup, and blowup [i.e., $L(z) = 0$ or $a^2(z) + b^2(z) = 0$] appears to occur when $V(z) = 0$ (i.e., whole-beam collapse).

The logical failure of the above conclusions occurs because the variance identity holds only so long as the beam does not blow up. Therefore the correct conclusion from the variance identity is that, when $H_0 < 0$, the beam blows up at some finite distance z_c such that $z_c \leq z^*$. In fact, NLS simulations show that blowup always occurs at $z_c < z^*$ (see, e.g., Fig. 3). This observation follows, for example, from the well-known Dawes–Marburger formula for the location of the blowup point of Gaussian beams, $\psi_0 = c \exp(-r^2/2)$ (Refs. 7 and 20):

$$z_c = 0.184[(p^{1/2} - 0.852)^2 - 0.0219]^{-1/2}, \quad p = N_0/N_{cr}, \quad (11)$$

which has 10% relative accuracy, as well as from the more accurate formula²¹ [Eq. (3.43) of Ref. 13]

$$z_c = 0.317(p - 1)^{-0.6346}, \quad (12)$$

which has a relative accuracy of 1%. Figure 3 shows that the actual value of z_c is significantly smaller than the variance identity prediction for the location of the blowup point of Gaussian beams:

$$z^* = \left(\frac{1}{pN_c/2 - 1} \right)^{1/2} \quad (13)$$

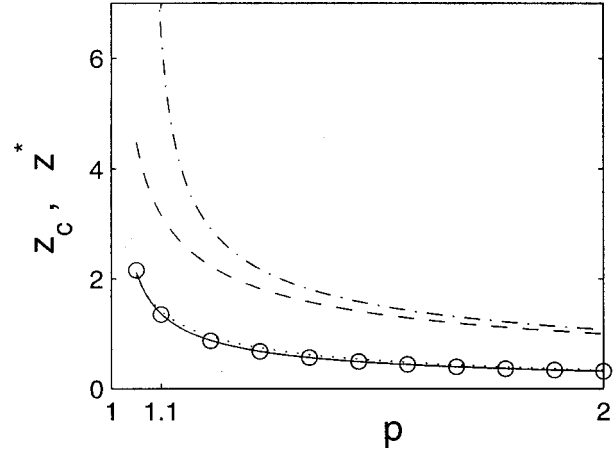


Fig. 3. Location of blowup as predicted by the variance identity [Eq. (13), dashed curve] and by the aberrationless approximation [Eq. (14), dashed-dotted curve] is significantly larger than the actual value (circles). Also shown are the curve-fitted Eqs. (11) (dotted curve) and (12) (solid curve).

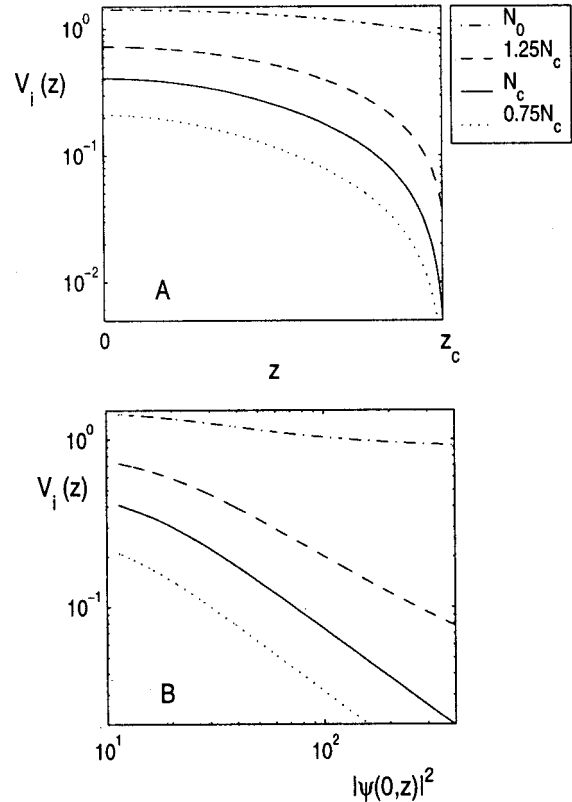


Fig. 4. Dynamics of V_i for the circular input beam $\psi(r, 0) = 2\sqrt{1.527N_{cr}} \exp(-r^2)$ (i.e., $P_0 = 1.5P_{circular}$, $H_0 = -2.4$). Here $N_i = 0.75N_{cr}$, N_{cr} , $1.25N_{cr}$, $N_0 \approx 1.52N_{cr}$, and $z_c \approx 0.23$.

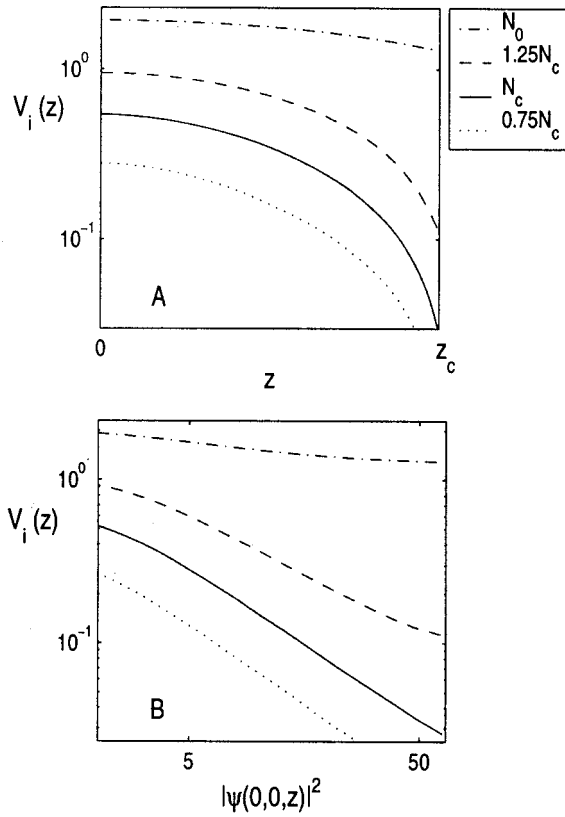


Fig. 5. Same as Fig. 4 but for the *elliptic* input beam $\psi(x, y) = 2\sqrt{1.19N_{cr}} \exp[-(x/1.3)^2 - y^2]$ [i.e., $P_0 = 1.5P_{cr}(1.3)$, $H_0 = -1.8$] and $z_c \approx 0.30$.

as well as from the aberrationless approximation prediction

$$z^* = \left(\frac{1}{p-1} \right)^{1/2}. \quad (14)$$

Inasmuch as $z_c < z^*$, the variance identity implies that at the blowup point z_c the variance is positive rather than zero. Therefore we can conclude that collapse is always a partial-beam process rather than a whole-beam process, regardless of whether H_0 is positive or negative. The inability of the aberrationless approximation to capture the partial-beam collapse is related to many of its misleading predictions [such as those that follow Eq. (10)].

One can only speculate as to why these misinterpretation of the consequences of the variance identity have persisted for so many years. One reason may be that, in the case of circular Gaussian input beams, the difference between the actual critical power and the power derived from the condition $H_0 = 0$ is only 5%.¹² Another reason is that the aberrationless approximation was considered to be an approximation rather than an assumption.

Although such has not been rigorously proved, NLS analysis and simulations strongly suggest that the power collapsing toward the beam axis is always equal to N_{cr} . To compare this property for circular and elliptic beams, let us define $V_i(z)$ to be the variance of the part of the beam with power N_i .²² Thus whole-beam collapse corre-

sponds to $V_i(z_c) = 0$ for all N_i . In contrast, if the amount of power going into the beam center is equal to N_{cr} , then

$$\begin{aligned} V_i(z_c) &= 0, & N_i &\leq N_{cr}, \\ V_i(z_c) &> 0, & N_i &> N_{cr}. \end{aligned} \quad (15)$$

In particular, $V(z_c) = V_0(z_c) > 0$. The results in Figs. 4 and 5 are clearly in agreement with expressions (15), showing that blowup for both circular and elliptic input beams (even with a negative Hamiltonian) is partial, with power N_{cr} . Additional numerical and analytic support for the fact that the collapsing power is always equal to N_{cr} is given in Section 4.

4. PARTIAL-BEAM COLLAPSE WITH A CIRCULAR TOWNESIAN PROFILE

To follow the dynamics of a self-focusing elliptic beam, we would like to recover the normalized beam widths $a(z)$ and $b(z)$ from NLS simulations. Under the assumption of aberrationless propagation, i.e.,

$$|\psi|^2 = \frac{1}{a(z)b(z)} F\left[\frac{x}{a(z)}, \frac{y}{b(z)}\right],$$

we can do this by using

$$\begin{aligned} a(z) &= \left[\frac{c^*}{\int |(|\psi|^2)_x| dx dy} \right]^{1/2}, \\ b(z) &= \left[\frac{c^*}{\int |(|\psi|^2)_y| dx dy} \right]^{1/2}, \end{aligned} \quad (16)$$

where

$$c^* = \left[\int |(|\psi_0|^2)_x| dx dy \right]^{1/2} \left[\int |(|\psi_0|^2)_y| dx dy \right]^{1/2}.$$

In the case of partial-beam collapse the whole-beam approach of Eqs. (16) should be modified, because a and b are the widths of the collapsing part of the beam whereas the calculation in Eqs. (16) is over the entire beam cross section. Therefore a more accurate way to recover a and b is with

$$\begin{aligned} a(z) &= \left[\frac{c^*}{\int_{\Omega(z)} |(|\psi|^2)_x| dx dy} \right]^{1/2}, \\ b(z) &= \left[\frac{c^*}{\int_{\Omega(z)} |(|\psi|^2)_y| dx dy} \right]^{1/2}, \end{aligned} \quad (17)$$

where

$$c^* = \left[\int_{\Omega_0} |(|\psi_0|^2)_x| dx dy \right]^{1/2} \left[\int_{\Omega_0} |(|\psi_0|^2)_y| dx dy \right]^{1/2}.$$

The integration domain $\Omega(z)$ is chosen such that it corresponds to the collapsing part of the beam. For example, in our simulations we use $\Omega(z) = \tilde{L}(z)\Omega_0$, where $\tilde{L}(z) = |\psi_0(0,0)/\psi(0,0,z)|$ and $\Omega_0 = \{(x, y) | -4.5 \leq x, y \leq 4.5\}$.

In Figs. 6 and 7 we plot the evolution of a/b as a function of normalized on-axis intensity and axial distance, respectively. First we note the difference between the values of a/b recovered with Eqs. (16) and (17), which provides further support that collapse is partial and not whole beam. As the collapsing power is always equal to N_c , at higher input powers the noncollapsing part of the beam has more power, explaining why the difference between Eqs. (16) and (17) increases as the input power is raised. Because we are interested in the widths of the collapsing part of the beam, from now on we recover a and b by using Eqs. (17).

At all input powers, near the blowup point the collapsing part of the beam approaches a circular profile, whereas at higher input powers it takes more focusing (and requires getting closer to the blowup point) to ap-

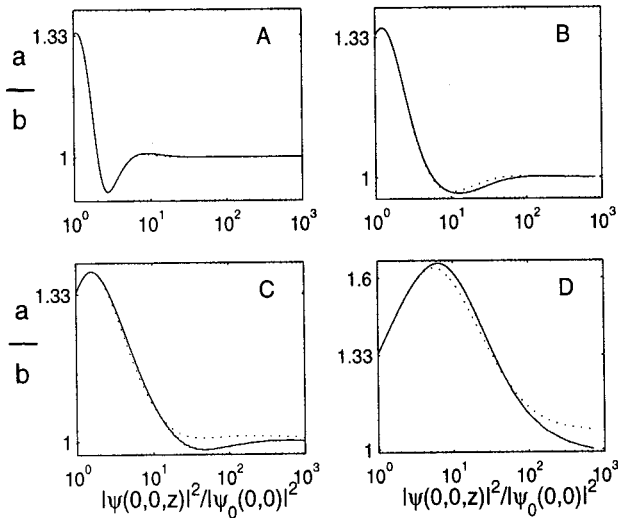


Fig. 6. Beam astigmatism as a function of normalized on-axis intensity, according to Eqs. (16) (dotted curves) and (17) (solid curves). Here $e = 1.3$, $\psi_0 = 2\sqrt{cP_{cr}(0)} \exp[-(x/e)^2 - y^2]$, and $P_{cr}(e) = 1.92P_{cr(circular)}$. A, $c = 0.839$, $P_0 = 1.1P_{cr}(e)$; B, $c = 1.144$, $P_0 = 1.5P_{cr}(e)$; C, $c = 1.525$, $P_0 = 2P_{cr}(e)$; D, $c = 3.05$, $P_0 = 4P_{cr}(e)$.

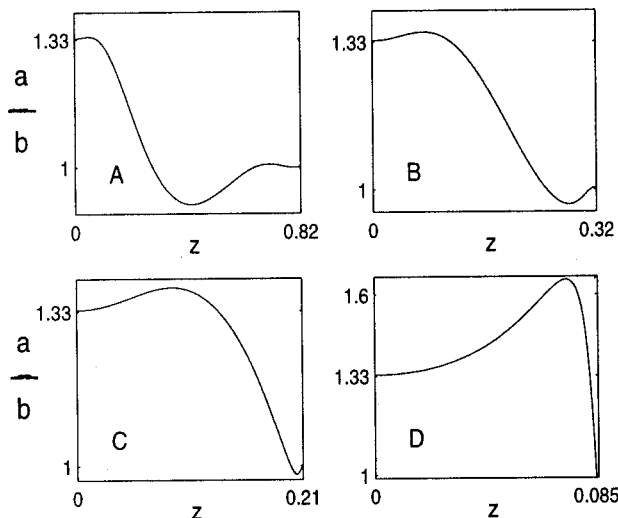


Fig. 7. Beam astigmatism as a function of axial distance for the correspondingly labeled parts of Fig. 6.

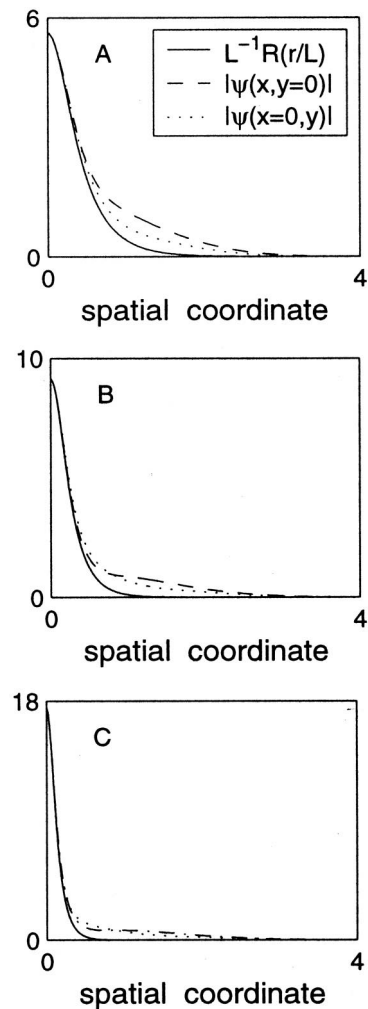


Fig. 8. Convergence of the collapsing part of an elliptic input beam to the circular Townes profile $L^{-1}(z)R(r/L(z))$. Here $\psi_0 = 2\sqrt{1.1646N_{cr}} \exp[-(3x/4)^2 - y^2]$ with $P_0 = 1.5P_{cr}(4/3)$ and $H_0 = -1.75$. Spatial coordinates: x (dashed curves), y (dotted curves), and r (solid curves). A, $z = 0.22$, $L = 0.52$; B, $z = 0.28$, $L = 0.32$; C, $z = 0.31$, $L = 0.165$.

proach a circular profile. We note that convergence to a circular profile was also observed in Refs. 11 and 23 and is consistent with self-focusing experiments with elliptic input beams, where it was found that “the damaged region was found to possess a circular rather than an elliptic cross section.”¹ Note that under the whole-beam definition [Eqs. (16)] a/b does not approach 1 (Figs. 6C and 6D), indicating that the noncollapsing part of the beam does not become circular.

Although this has not been rigorously proved, there is a substantial body of evidence that near the blowup point the collapsing part of the beam approaches a circular profile that is a modulated Townes soliton, i.e., $|\psi| \sim L^{-1}(z)R(r/L(z))$, where $L(z)$ is the normalized beam width. Our simulations confirm this asymptotic-profile property for input elliptic beams. For example, in Fig. 8 we see that, after focusing by a factor of 5, the beam profile in the vicinity of the z axis is already close to a modulated Townes profile. This asymptotic-profile property is consistent with expressions (15), and explains why the

collapsing power is always equal to N_{cr} . The existence of an asymptotic profile also explains the lines with slope ≈ -1 observed on a log-log scale in Figs. 4B and 5B when $N_i \leq N_{cr}$, because then

$$V_i \sim L^2(z)V_i(0) \sim V_i(0)R^2(0)|\psi(z, 0)|^{-2}.$$

We note that Fig. 8 also shows that the noncollapsing part of the beam does not become circular.

Because the Townes profile looks quite similar to a Gaussian profile it might seem that the aberrationless approximation can be a reasonable assumption for the advanced stages of the propagation. Such is not the case, however, because the Townesian profile has the unique property that diffraction and focusing Kerr nonlinearity completely balance each other. As a result, as the profile gets closer to a Townesian the propagation dynamics depends on the small difference between diffraction and nonlinearity, and small additional mechanisms that were neglected in the derivation of NLS from Maxwell equations, such as nonparaxiality,²⁴ time-dispersion,²⁵ and nonlinear saturation,²⁶ can have a large effect. These additional mechanisms can have a large effect even when they are small compared with the diffraction and nonlinear terms, precisely because they compete against the small difference between Kerr nonlinearity and diffraction, rather than separately against diffraction and nonlinearity.¹³ The inability of the aberrationless approximation to capture this delicate balance is its second major weakness.

5. TWO-STAGE APPROACH: AN ALTERNATIVE TO THE ABERRATIONLESS APPROXIMATION

As we have seen, the failure of the aberrationless approximation results from its inability to model the partial blowup feature during the early stage of the propagation and from the subsequent delicate balance between Kerr nonlinearity and diffraction. Based on the results of the previous sections we can, however, propose an alternative two-stage approach to analyzing the propagation of elliptic beams:

First stage: The first stage of the propagation lasts until the beam gets close to the focal point²⁷ and moderate focusing has taken place. During this stage the collapsing part of the beam changes from elliptic to a circular Townes profile. Small additional mechanisms, which were neglected in the derivation of the NLS from Maxwell equations, have a relatively small effect during this stage. Therefore this part of the propagation can be modeled by the unperturbed NLS [Eq. (4)].

Second stage: The second stage of the propagation occurs when the beam is near and beyond the blowup point. During this stage the focused part of the beam is close to a circular Townes soliton. As a result, small additional mechanisms can have large effects on the beam propagation, and these effects are the same as in the case of circular beams. Therefore these effects can be analyzed by use of modulation theory^{13,28} which is based on perturbations about the Townes profile and provides a systematic method for deriving reduced equations that are independent of the transverse (x, y) coordinates.

We have already seen that the two-stage approach describes self-focusing of elliptic beams governed by the NLS model [Eq. (4)]. We now show how this approach can be used to analyze the propagation of elliptic beams in the presence of additional mechanisms.

A. Saturating Nonlinearity

The propagation of elliptic beams in a medium with saturable nonlinearity can be modeled by

$$i\psi_z(x, y, z) + \Delta_{\perp}\psi + \frac{|\psi|^2}{1 + \epsilon|\psi|^2}\psi = 0, \quad 0 < \epsilon \ll 1. \quad (18)$$

In Ref. 3 it was concluded, based on the aberrationless approximation, that in this case “stationary self-trapping is forbidden,” in contrast to the case of elliptic beams in a medium with a Kerr nonlinearity for which, based on the aberrationless approximation, it was predicted that the “self-trapping regime [will be given by] $H_0 = 0$.”² In fact, both predictions are wrong. There are no self-trapping solutions of the nonsaturated NLS [Eq. (4)], except for the waveguide solutions [Eqs. (6)], which have precisely the critical power and are known to be

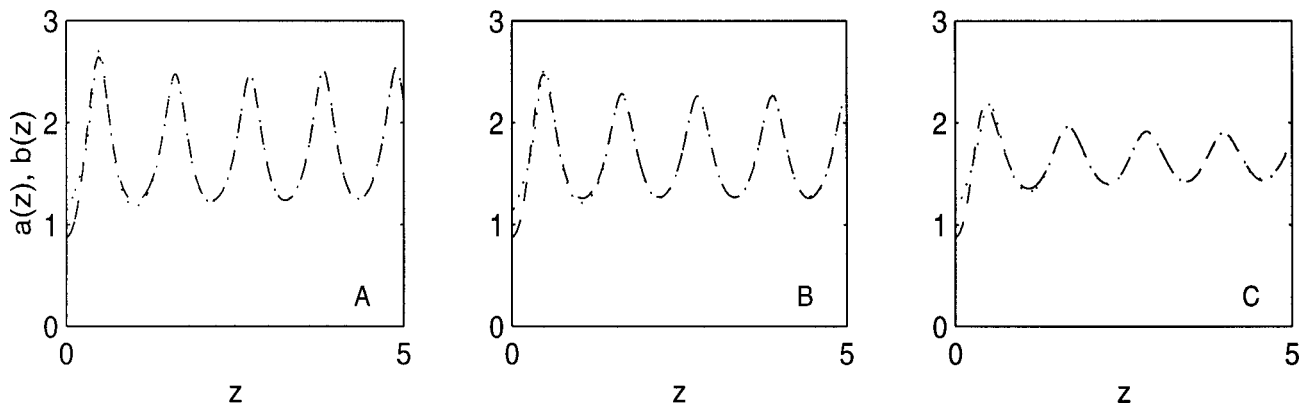


Fig. 9. Beam widths in the x direction [$a(z)$, dotted curves] and the y direction [$b(z)$, dashed curves] for the elliptic beam $\psi_0(x, y) = 2\sqrt{1.91N_{cr}}\exp[-(x/1.3)^2 - y^2]$, with $P_0 = 1.5P_{cr}(1.3)$, propagating in media with saturating-nonlinearity parameter $\epsilon = 0.01$. The equations that govern propagation are A, Eq. (18); B, Eq. (19); C, Eq. (20).

unstable.¹⁵ All other solutions with power above critical undergo collapse, whereas those with power below critical go through a single focusing–defocusing event (see Fig. 1). In contrast, elliptic beams propagating in a medium with saturable nonlinearity can undergo almost periodic focusing–defocusing oscillations (Fig. 9A), which are reminiscent of the propagation pattern observed in cw self-trapping experiments.²⁹

The results in Fig. 9A agree with the two-stage approach to self-focusing of elliptic beams. The first stage lasts approximately one cycle, during which the collapsing part of the beam becomes circular. Therefore, further propagation can be analyzed by application of modulation theory to Eq. (18). Doing so results in a reduced equation, which shows that beams with input power moderately above N_{cr} undergo focusing–defocusing oscillations,^{13,28} as indeed we can observe from Fig. 9A.

Another prediction of modulation theory (see proposition 5.1 in Ref. 13) is that the leading-order effect of saturation is the same, regardless of whether one models saturation by using Eq. (18):

$$i\psi_z(x, y, z) + \Delta_{\perp}\psi + \frac{1 - \exp(-2\epsilon|\psi|^2)}{2\epsilon}\psi = 0 \quad (19)$$

or

$$i\psi_z(x, y, z) + \Delta_{\perp}\psi + |\psi|^2\psi - \epsilon|\psi|^4\psi = 0. \quad (20)$$

Therefore, based on the two-stage approach, we can predict that elliptic beams propagating in a medium with saturating nonlinearities given by relation (19) or Eq. (20) will also become circular and undergo focusing–defocusing cycles, just as in the case of Eq. (18). The simulation results in Figs. 9B and 9C confirm this prediction.

B. Nonparaxiality

The NLS as the model equation for laser beam propagation through a Kerr medium is derived from the scalar Helmholtz equation for the electric field E :

$$\left(\Delta_{\perp} + \frac{\partial^2}{\partial z^2}\right)E(x, y, z) + k^2E = 0, \\ k^2 = k_0^2\left(1 + \frac{2n_2}{n_0}|E|^2\right).$$

To make this derivation, one introduces the slowly varying envelope form $E = \psi \exp(ik_0z)$ for the electric field to get the nondimensional form of the Helmholtz equation:

$$\epsilon\psi_{zz} + i\psi_z + \Delta_{\perp}\psi + |\psi|^2\psi = 0, \quad \epsilon = \left(\frac{\lambda}{4\pi r_0}\right)^2. \quad (21)$$

Because beam wavelength λ is much smaller than initial beam radius r_0 , it follows that $0 < \epsilon \ll 1$. This suggests that $\epsilon\psi_{zz}$ can be neglected, in which case Eq. (21) reduces to the NLS [Eq. (4)].

Neglecting $\epsilon\psi_{zz}$ is called the paraxial approximation or the parabolic approximation. This approximation is valid for rays that propagate almost parallel to the z axis, but it breaks down near the focal point. Feit and Fleck,³⁰ and later Akhmediev and Soto-Crespo^{31,32} showed numerically that nonparaxiality arrests the collapse of cir-

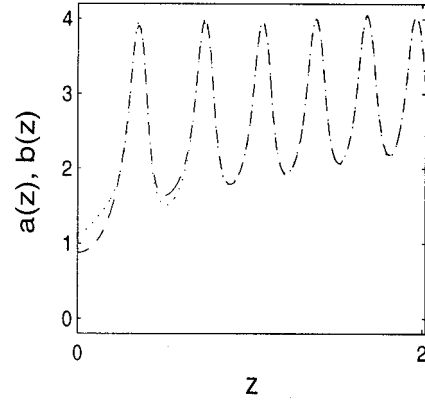


Fig. 10. Same as Fig. 9 but for propagation in the presence of nonparaxial effects [Eq. (22) with $\epsilon = 0.0025$].

cular beams, leading instead to focusing–defocusing cycles. Fibich²⁴ used modulation theory to show analytically that nonparaxiality arrests self-focusing and leads to focusing–defocusing oscillations and that, throughout the beam propagation, nonparaxiality remains small compared with diffraction and the Kerr nonlinearity.

Based on the two-stage approach, we expect elliptic input beams that are propagating in the presence of small nonparaxiality first to undergo partial beam collapse, during which they approach a circular Townesian profile, and then to go through focusing–defocusing cycles. Unfortunately, at present it is not possible to compare this prediction with simulations of Eq. (21), because Eq. (21) is a nonlinear boundary-value problem that includes back-scattering. Therefore we adopt the standard approach to solving Eq. (21) numerically, which is to replace that equation with an evolution equation for the forward-propagation wave. Mathematically, this amounts to replacing the $\epsilon\psi_{zz}$ term with terms that involve only spatial derivatives (see, e.g., Ref. 33). The resultant modified equation for propagation in the presence of weak nonparaxiality, which differs from Eq. (21) only in $O(\epsilon^2)$ terms, is

$$i\psi_z + \Delta_{\perp}\psi + |\psi|^2\psi = \epsilon[\Delta_{\perp}^2\psi + 4|\psi|^2\Delta_{\perp}\psi + 4|\nabla_{\perp}\psi|^2\psi + 2(\nabla_{\perp}\psi)^2\psi^* + |\psi|^4\psi]. \quad (22)$$

In Fig. 10 we present simulations of Eq. (22) that confirm the prediction of the two-stage approach: The beam undergoes focusing–defocusing oscillations, and the inner part of the beam becomes circular after two cycles.

C. Normal Time Dispersion

The propagation of ultrashort elliptic pulses in a medium with normal (positive) group-velocity dispersion is modeled by

$$i\psi_z(x, y, z, t) + \Delta_{\perp}\psi - \frac{L_{df}k_{\omega\omega}}{T^2}\psi_{tt} + |\psi|^2\psi = 0,$$

where T is the pulse duration and $k_{\omega\omega} > 0$ is the normal group-velocity dispersion. In Ref. 4 it was concluded, based on the aberrationless approximation, that “for positive group-velocity dispersion and only moderate astigmatism, there is a minimum pulse duration below which the spatial collapse is completely prevented at any input

power.” Our approach predicts a different outcome, as follows: During the first stage of the propagation the pulse self-focuses while it approaches a circular Townesian profile. From this point, further propagation is similar to that of circular beams. We recall that the critical power for circular ultrashort pulses increases with normal group-velocity dispersion but that this increase is finite rather than infinite.³⁴ In addition, based on modulation theory, it was predicted in Ref. 35 that the collapse of ultrashort pulses whose power is moderately above this critical power will involve asymmetric pulse splitting, a prediction that was confirmed both experimentally and numerically in Refs. 36 and 37. Therefore we predict that sufficiently intense³⁸ ultrashort elliptic pulses will also collapse while they are undergoing asymmetric pulse splitting. Whether this prediction or the one in Ref. 4 is correct, however, can be determined only either by comparison with simulations of the time-dispersive NLS or by experiments.

6. FINAL REMARK

The aberrationless approximation leads to a significant simplification in the analysis of the propagation of laser beams in Kerr media. Unfortunately, the results of this study show that, in the case of elliptic beams, application of the aberrationless approximation can lead to highly inaccurate quantitative predictions as well as to qualitative predictions that are simply wrong. As we have seen, this failure of the aberrationless approximation is related to its inability to capture the partial blowup process during the first stage of the propagation and the subsequent delicate balance between diffraction and nonlinearity, which gives rise to the large effect of small mechanisms. As these deficiencies of the aberrationless approximation are not related to beam ellipticity, our criticism of the aberrationless approximation applies also to the case of circular beams. Obviously, not all predictions of the aberrationless approximation are incorrect or inaccurate. However, *a priori* (i.e., before comparison with NLS simulations), it is not possible to know which predictions will turn out to be correct and which will not. In addition, the choice of profile function in the aberrationless approximation seems to be *ad hoc* and to vary with application. Therefore it is also not clear, *a priori*, which profile function should be used.

The above discussion suggests that, ideally, one should always compare predictions based on the aberrationless approximation with numerical simulations of the NLS. In some cases, comparison with numerical simulations is not easy. For example, in the case of ultrashort elliptic beams (Subsection 5.C), such a comparison requires solving the NLS in $(3 + 1)$ dimensions. In that case, one may consider a comparison with experiments (as was done in Ref. 39). However, in the case of elliptic cw beams, and even more so in the case of cw circular beams, there is no real difficulty in solving the NLS numerically.

In this paper we have presented a two-stage approach to analyzing the propagation of elliptic beams. Unlike for the aberrationless approximation, predictions based on the two-stage approach seem to be in good agreement with NLS simulations. This approach applies also to cir-

cular beams, the only difference being that, during the first stage, the collapsing part of the beam approaches the Townes profile while maintaining a circular profile. The validity of this approach for circular beams is manifested by the success of predictions of modulation theory for beam propagation in the presence of various small mechanisms.¹³

ACKNOWLEDGMENTS

We acknowledge useful discussions with A. Gaeta as well as helpful suggestions by the referees of an earlier version of this paper. This research was supported by grant 97-00127 from the United States–Israel Binational Science Foundation, Jerusalem, Israel.

REFERENCES AND NOTES

1. C. R. Giuliano, J. H. Marburger, and A. Yariv, “Enhancement of self-focusing threshold in sapphire with elliptical beams,” *Appl. Phys. Lett.* **32**, 58–60 (1972).
2. F. Cornolti, M. Lucchesi, and B. Zambon, “Elliptic Gaussian beam self-focusing in nonlinear media,” *Opt. Commun.* **75**, 129–135 (1990).
3. S. Konar and A. Sengupta, “Propagation of an elliptic Gaussian laser beam in a medium with saturable nonlinearity,” *J. Opt. Soc. Am. B* **11**, 1644–1646 (1994).
4. G. Cerullo, A. Dienes, and V. Magni, “Space–time coupling and collapse threshold for femtosecond pulses in dispersive nonlinear media,” *Opt. Lett.* **21**, 65–67 (1996).
5. T. Singh and S. S. Kaul, “Self-focusing and self-phase modulation of elliptic Gaussian laser beam in a graded Kerr-medium,” *Indian J. Pure Appl. Phys.* **11**, 794–797 (1999).
6. S. A. Akhmanov, A. P. Sukhorukov, and R. V. Khokhlov, “Self-focusing and self-trapping of intense light beams in a nonlinear medium,” *JETP* **23**, 1025–1033 (1966).
7. J. H. Marburger, “Self-focusing: theory,” *Prog. Quantum Electron.* **4**, 85–110 (1975).
8. D. Anderson, M. Bonnedal, and M. Lisak, “Self-trapped cylindrical laser beams,” *Phys. Fluids* **22**, 1838–1840 (1979).
9. M. Desaix, D. Anderson, and M. Lisak, “Variational approach to collapse of optical pulses,” *J. Opt. Soc. Am. B* **8**, 2082–2086 (1991).
10. M. Karlsson, “Optical beams in saturable self-focusing media,” *Phys. Rev. A* **46**, 2726–2734 (1992).
11. B. Gross and J. T. Manassah, “Numerical solution for the propagation of an elliptic Gaussian beam in a Kerr medium,” *Phys. Lett. A* **169**, 371–378 (1992).
12. G. Fibich and A. Gaeta, “Critical power for self-focusing in bulk media and in hollow waveguides,” *Opt. Lett.* **25**, 335–337 (2000).
13. G. Fibich and G. C. Papanicolaou, “Self-focusing in the perturbed and unperturbed nonlinear Schrödinger equation in critical dimension,” *SIAM (Soc. Ind. Appl. Math.) J. Appl. Math.* **60**, 183–240 (1999).
14. C. Sulem and P. L. Sulem, *The Nonlinear Schrödinger Equation* (Springer, New York, 1999).
15. M. I. Weinstein, “Nonlinear Schrödinger equations and sharp interpolation estimates,” *Commun. Math. Phys.* **87**, 567–576 (1983).
16. V. I. Talanov, “Focusing of light in cubic media,” *JETP Lett.* **11**, 199–201 (1970).
17. The values of e can be recovered by use of the equation $e = 1 \pm \sqrt{h^2 - 1}$.
18. The relative error of relation (9) is less than 1.5% in the range $1/2.5 \leq e \leq 2.5$.

19. S. N. Vlasov, V. A. Petrishchev, and V. I. Talanov, "Averaged description of wave beams in linear and nonlinear media," *Izv. Vyssh. Uchebn. Zaved. Radiofiz.* **14**, 1353–1363 (1971) [*Radiophys. Quantum Electron.* **14**, 1062–1070 (1971)].
20. E. L. Dawes and J. H. Marburger, "Computer studies in self-focusing," *Phys. Rev.* **179**, 862–868 (1969).
21. The value of z_c here is twice that given in Eq. (13) below, because there $\psi_0 = c \exp(-r^2)$.
22. I.e., if $\int_{\sqrt{x^2+y^2} \leq r_i(z)} |\psi|^2 dx dy = N_i$, then $V_i(z) = \int_{\sqrt{x^2+y^2} \leq r_i(z)} |\psi|^2 dx dy$.
23. M. J. Landman, G. C. Papanicolaou, C. Sulem, P. L. Sulem, and X. P. Wang, "Stability of isotropic singularities for the nonlinear Schrödinger equation," *Physica D* **47**, 393–415 (1991).
24. G. Fibich, "Small beam nonparaxiality arrests self-focusing of optical beams," *Phys. Rev.* **76**, 4356–4359 (1996).
25. G. Fibich, V. M. Malkin, and G. C. Papanicolaou, "Beam self-focusing in the presence of small normal time dispersion," *Phys. Rev. A* **52**, 4218–4228 (1995).
26. V. M. Malkin, "On the analytical theory for stationary self-focusing of radiation," *Physica D* **64**, 251–266 (1993).
27. I.e., the location of blowup in the unperturbed NLS [Eq. (4)].
28. G. Fibich and G. C. Papanicolaou, "A modulation method for self-focusing in the perturbed critical nonlinear Schrödinger equation," *Phys. Lett. A* **239**, 167–173 (1998).
29. J. E. Bjorkholm and A. Ashkin, "cw self-focusing and self-trapping of light in sodium vapor," *Phys. Rev. Lett.* **32**, 129–132 (1974).
30. M. D. Feit and J. A. Fleck, "Beam nonparaxiality, filament formation, and beam breakup in the self-focusing of optical beams," *J. Opt. Soc. Am. B* **5**, 633–640 (1988).
31. N. N. Akhmediev and J. M. Soto-Crespo, "Generation of a train of three-dimensional optical solitons in a self-focusing medium," *Phys. Rev. A* **47**, 1358–1364 (1993).
32. J. M. Soto-Crespo and N. N. Akhmediev, "Description of the self-focusing and collapse effects by a modified nonlinear Schrödinger equation," *Opt. Commun.* **101**, 223–230 (1993).
33. S. Chi and Q. Guo, "Vector theory of self-focusing of an optical beam in Kerr media," *Opt. Lett.* **20**, 1598–1560 (1995).
34. G. G. Luther, A. C. Newell, J. V. Moloney, and E. M. Wright, "Self-focusing threshold in normally dispersive media," *Opt. Lett.* **19**, 862–864 (1994).
35. G. Fibich and G. C. Papanicolaou, "Self-focusing in the presence of small time dispersion and nonparaxiality," *Opt. Lett.* **22**, 1379–1381 (1997).
36. J. K. Ranka and A. L. Gaeta, "Breakdown of the slowly varying envelope approximation in the self-focusing of ultrashort pulses," *Opt. Lett.* **23**, 534–536 (1998).
37. S. A. Diddams, H. K. Eaton, A. A. Zozulya, and T. S. Clement, "Amplitude and phase measurements of femtosecond pulse splitting in nonlinear dispersive media," *Opt. Lett.* **23**, 379–381 (1998).
38. Clearly, the critical power for collapse of ultrashort elliptical pulses should be higher than for circular pulses.
39. V. Magni, G. Cerullo, S. De Silvestri, and A. Monguzzi, "Astigmatism in Gaussian-beam self-focusing and in resonators for Kerr-lens mode locking," *J. Opt. Soc. Am. B* **12**, 476–485 (1995).